Highly Ordered TiO_2 Nanotubes on Patterned Substrates: Synthesis-in-Place for Ultrasensitive Chemiresistors

Do Hong Kim †, Young-Seok Shim ‖, Hi Gyu Moon ‖, Hye Jung Chang ‡, Dong Su §, Soo Young Kim ¶, Jin-Sang Kim ‖, Byeong Kwon Ju ⊥, Seok-Jin Yoon ‖, and Ho Won Jang *†

† Department of Materials Science and Engineering, Research Institute of Advanced Materials, Seoul National University, Seoul 151-744, Korea

‡ Nanomaterials Analysis Center, Korea Institute of Science and Technology, Seoul 136-791, Korea

§ Center for Functional Nanomaterials, Brookhaven National Laboratory, Upton, New York 11973, United States

‖ Electronic Materials Research Center, Korea Institute of Science and Technology, Seoul 136-791, Korea

⊥ Display and Nanosystem Laboratory, College of Engineering, Korea University, Seoul 136-361, Korea

¶ School of Chemical Engineering and Materials Science, Chung-Ang University, Seoul 156-756, Korea

J. Phys. Chem. C, 2013, *117* (34), pp 17824-17831

DOI: 10.1021/jp405150b

Publication Date (Web): August 1, 2013

ACS ActiveView PDF
Hi-Res Print, Annotate, Reference QuickView

PDF [1276 KB]

PDF w/ Links[492 KB]

Full Text HTML

Abstract

Supporting Info ->

Figures

Reference QuickView

Add to ACS ChemWorx

Tools

Add to Favorites

Download Citation

Permalink

Order Reprints

Rights & Permissions

Citation Alerts

SciFinder Links

SciFinder

Get Reference Detail

Get Substances

Get Cited

Explore by:

Author of this Article

Any Author

Research Topic

Related Content

Other ACS content by these authors:

Do Hong Kim

Young-Seok Shim

Hi Gyu Moon

Hye Jung Chang

Dong Su

Soo Young Kim

Jin-Sang Kim

Byeong Kwon Ju

Seok-Jin Yoon

Ho Won Jang

THE JOURNAL OF PHYSICAL CHEMISTRY C

Article

pubs.acs.org/JPCC

Highly Ordered TiO_2 Nanotubes on Patterned Substrates: Synthesis-in-Place for Ultrasensitive Chemiresistors

Do Hong Kim,[†] Young-Seok Shim,[∥] Hi Gyu Moon,[∥] Hye Jung Chang,[‡] Dong Su,[§] Soo Young Kim,[¶] Jin-Sang Kim,[∥] Byeong Kwon Ju,[⊥] Seok-Jin Yoon,[∥] and Ho Won Jang*[,†]

[†]Department of Materials Science and Engineering, Research Institute of Advanced Materials, Seoul National University, Seoul 151-744, Korea

[‡]Nanomaterials Analysis Center, Korea Institute of Science and Technology, Seoul 136-791, Korea

[§]Center for Functional Nanomaterials, Brookhaven National Laboratory, Upton, New York 11973, United States

[∥]Electronic Materials Research Center, Korea Institute of Science and Technology, Seoul 136-791, Korea

[⊥]Display and Nanosystem Laboratory, College of Engineering, Korea University, Seoul 136-361, Korea

[¶]School of Chemical Engineering and Materials Science, Chung-Ang University, Seoul 156-756, Korea

Supporting Information

ABSTRACT: Integrating a highly ordered TiO_2 nanotube array with patterned substrates is an effective design strategy for taking advantage of one-dimensional nanotube structures such as high surface-to-volume ratio and novel functionalities of TiO_2, but many challenges remain in synthesis. Here we report a novel synthesis-in-place method for highly ordered vertical TiO_2 nanotube films on various patterned substrates and the application of the films to chemiresistive sensors. A unique synthetic strategy, in which the Pt bottom electrodes were clamped during anodization, leads to the complete anodization of the Ti layer to TiO_2 nanotubes not only on SiO_2/Si substrates but also on glass and sapphire substrates, which can be used as chemiresistors without additional processes. TiO_2 nanotube sensors on SiO_2/Si substrates show unprecedentedly ultrahigh responses to ethanol and acetone with detection limits down to parts per billion levels. Beyond the high sensitivity, selective responses to ethanol and acetone create opportunities for application in breath analyzers to diagnose human respiratory diseases.

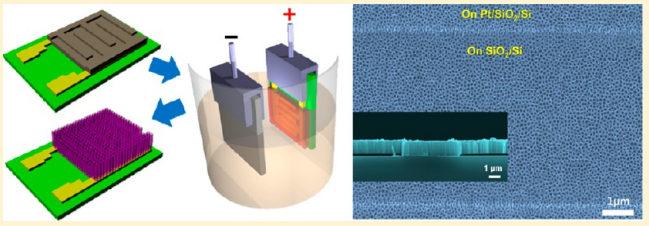

Titanium dioxide (TiO_2) is one of the most attractive materials in transition metal oxides owing to high chemical stability, strong photocatalytic effects, low cost, and nontoxicity.[1−3] It has a wide variety of applications such as dye-sensitized solar cells,[4−6] photoelectrochemical water splitting,[7−9] antireflection coatings,[10−12] Li-ion batteries,[13−15] and chemiresistors.[16−18] For these applications, since the device performance rests largely on the surface-to-volume ratio of the material, tremendous efforts have been devoted to synthesize TiO_2 nanomaterials including nanoparticles, nanowires, nanorods, nanobelts, nanosheets, nanosponges, and nanotubes.[19−28] Among them, TiO_2 nanotubes have been extensively studied because of the ease of anodic oxidation processes for the formation of self-ordered nanotubular arrays.[29−33] Particularly, they have extremely large specific surface areas compared with plain films and show excellent adsorption and desorption of chemical vapors, which are desirable for high performance chemiresistors.[34,35]

Of the two main approaches to fabricate chemiresistors based on TiO_2 nanotubes, the first is the direct anodization of Ti foils. Resultant TiO_2 nanotube arrays on Ti substrates can act as chemical sensing layers with high sensitivity to formaldehyde, acetone, and ethanol at room temperature.[36] In addition, high sensitivity to H_2 has been reported from Pd-doped TiO_2 nanotube arrays.[37] Nonetheless, such nanotube arrays have not been exploited for chemiresistors operating at elevated temperatures for the detection of a wide variety of chemical vapors because the conducting Ti substrates easily form electrical shorts with the sensor electrodes. In addition, the Ti substrates are not compatible with high-throughput semiconductor fabrication processes. The second approach is the use of the hydrothermal method to synthesize porous TiO_2 nanotubes. Porous TiO_2 nanotube sensors have been reported to have improved response and selectivity to toluene at high temperatures.[38] In this method, however, active sensing layers are composed of randomly distributed TiO_2 nanotubes, and thus the intrinsic large surface area of TiO_2 nanotubes cannot be fully utilized for vapor sensing, which leads to relatively lower sensitivities than sensors based on TiO_2 nanoparticles.

To overcome these problems, the anodization of Ti thin films on foreign substrates including Si, Al_2O_3, and glass is a desirable way to fabricate high performance chemiresistors

Received: May 24, 2013
Revised: July 20, 2013
Published: August 1, 2013

   dx.doi.org/10.1021/jp405150b | J. Phys. Chem. C 2013, 117, 17824−17831

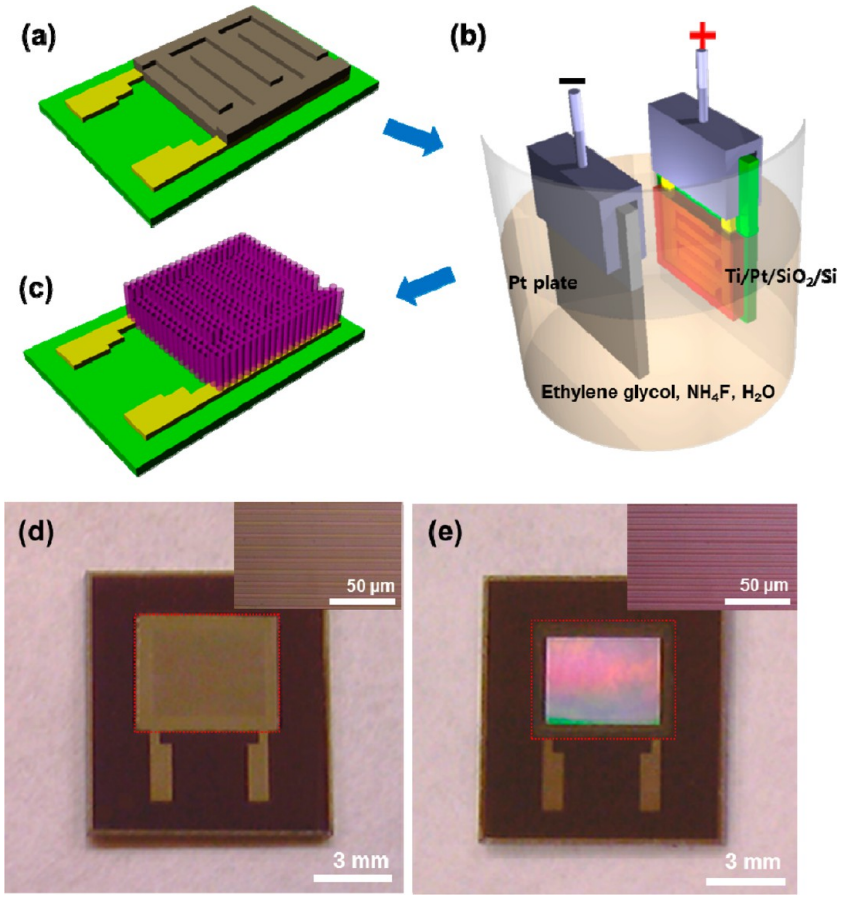

Figure 1. (a–c) Sketch illustrating our synthesis-in-place method to form TiO_2 nanotube films on Pt-IDE-patterned SiO_2/Si substrate. The key idea of our method is clamping the Pt IDEs as the current spreader during anodization. (d) Photograph of Ti film on Pt-IDE-patterned SiO_2/Si substrate before anodization. Inset: optical microphotograph of the 500-nm-thick Ti films on Pt-IDE-patterned SiO_2/Si substrate. (e) Photograph of TiO_2 nanotube film on Pt IDEs after anodization. Inset: optical microphotograph of TiO_2 nanotube sensors.

based on TiO_2 nanotubes, although some technological challenges remain to be solved. First, the quality of the TiO_2 nanotubes obtained by the anodization of Ti thin films is worse than that of those by the anodization of Ti foils.[39] Second, the clamped region for electrical contact remains Ti metal after anodization.[40] Third, complete anodization of the Ti layer into the TiO_2 layer is difficult due to the presence of potential gradients in the Ti layer during anodization.

In this article, we report the synthesis of highly ordered vertical TiO_2 nanotube thin films on various substrates, including Si, Al_2O_3, and glass, using anodization for sensor applications. The quality of the nanotube thin films is unparalleled with previous reports and comparable with those of TiO_2 thick films on Ti foil. We reveal that the crystallinity of initial Ti films is a critical factor determining the quality of the nanotube thin films. The diameter of the nanotubes is controlled by the applied voltage and is increased up to 160 nm with the applied voltage of 200 V, where the anodization time is as short as 90 s for obtaining 1-μm-thick nanotube thin films. Direct synthesis of TiO_2 nanotube thin films on Si substrates patterned with Pt electrodes leads to highly sensitive and selective sensors to acetone and ethanol vapors. The resulting detection limits down to several parts per billion levels suggest the great potential of TiO_2 nanotube thin film sensors for use in breath analyzers to diagnose human diseases noninvasively.

RESULTS AND DISCUSSION

Figure 1 shows a fabricated TiO_2 nanotube sensor for which a SiO_2/Si substrate with Pt interdigitated electrodes (IDEs) was used. Interspacing between Pt IDEs was 5 μm. The Ti film was deposited onto the IDEs by an electron beam evaporator, and then anodization was conducted in ethylene glycol and NH_4F-based electrolyte at room temperature, resulting in the formation of a TiO_2 nanotube film (Figure 1a–c). The key idea of our anodization method to realize the complete anodization of the whole region of the Ti film into a TiO_2 nanotube film is clamping the Pt IDEs for the anodization rather than the Ti film itself. Since current efficiently spreads though the Pt IDEs to the Ti film, potential gradients do not exist in the Ti layer during anodization, which leads to the uniform anodization of Ti to TiO_2. Especially when the thickness of the under Ti layer is thinner, the current spreading through Pt IDEs becomes more effective, resulting in the complete anodization of Ti. In addition, the SiO_2 layer acts as an oxidation stop layer, which enables the whole Ti layer to be converted to TiO_2 nanotubes. The photographs in Figure 1d,e clearly show that the shiny Ti film was changed to optically semitransparent TiO_2 film after anodization.

The grain shape and crystallinity of initial Ti films are critical for the formation of highly ordered TiO_2 nanotube films. When Ti film was deposited at room temperature, the film was formed by sequential stacking of several grains along the cross-section (Figure 2a). This leads to the formation of irregular nanotubes

dx.doi.org/10.1021/jp405150b | J. Phys. Chem. C 2013, 117, 17824–17831

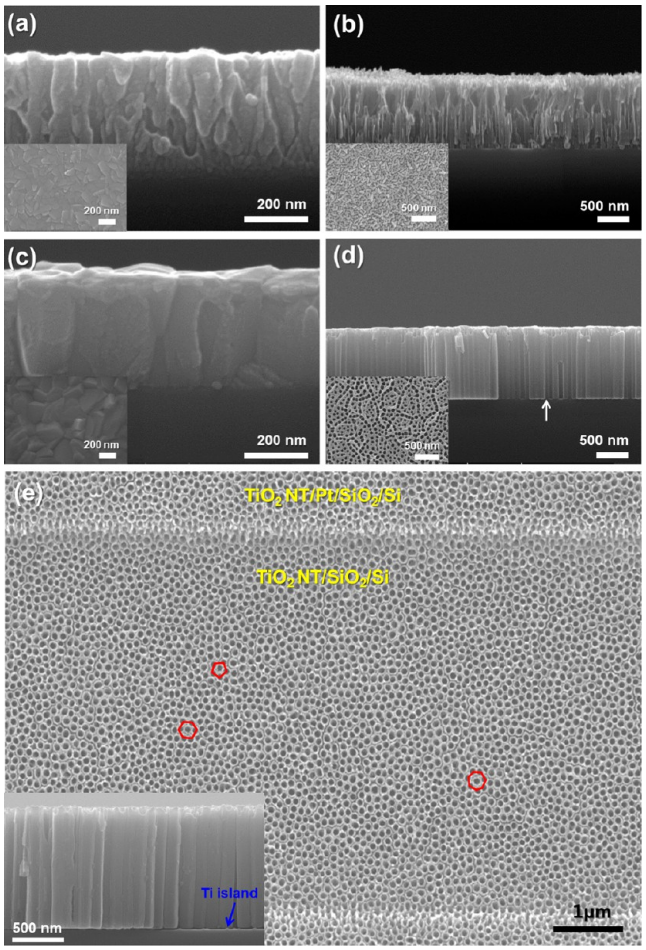

Figure 2. Cross-sectional SEM images of Ti films deposited onto a SiO_2/Si substrate at room temperature (a) before and (b) after anodization. The insets are plain-view SEM images. (c) Cross-sectional SEM images of the Ti films deposited at 600 °C. (d) Cross-sectional SEM images of the TiO_2 nanotubes formed by anodization of Ti film deposited at 600 °C. (e) Plain-view SEM images of TiO_2 nanotube films on Pt-IDE-patterned SiO_2/Si substrates after Ar ion etching. The inset in (e) shows the cross-sectional SEM image of TiO_2 nanotube films after Ar ion etching to remove the top layer.

with holes in the tube walls after anodization. Furthermore, relatively large pores by the merging of several nanotubes together were observed (Figure 2b). When the Ti film was evaporated at 600 °C, the film was observed to be highly textured with columnar grains, as shown in Figure 2c. However, using the Scherrer equation, the grain size of both films was almost the same (20–40 nm). From the X-ray diffraction (XRD) measurements, we observed that the microstructure of the Ti film deposited at 600 °C was very close to that of bulk Ti (JCPDS #44-1294), while the Ti film deposited at room temperature showed a quite different microstructure (Figure S1, Supporting Information). After anodization, the TiO_2 nanotubes were perfectly vertical and highly ordered with uniform diameters (Figure 2d). The Ti films were completely anodized to TiO_2 nanotubes on both SiO_2 and Pt electrodes (Figure S2, Supporting Information). There was no significant difference in the quality of TiO_2 nanotubes. This indicates that the crystallinity of the initial Ti film strongly influences the formation of TiO_2 nanotubes. To the best of our knowledge, no previous studies on well-ordered TiO_2 nanotube thin films have been published. A random pore oxide layer exists on the surface of TiO_2 nanotube films due to the anodic current drop at the initial stage of the anodization.[41] This layer can prevent diffusion and adsorption of gas molecules into the underlying nanotubes and thus degrade device performance. We applied Ar ion etching for effective removal of the surface layer. Figure 2e shows the surface of the highly ordered TiO_2 nanotube film after removal of the surface layer. The surface of the nanotubes consists mainly of close-packed hexagonal structure, but partially pentagon and heptagon are also observed. In addition, the cross-sectional image in the inset of Figure 1e clearly shows the remaining Ti islands (~10 nm) owing to the rounded oxide tube bottoms. In addition to Si substrates, we could synthesize high-quality vertical TiO_2 nanotube films on various substrates including indium tin oxide (ITO)/glass, fluorine-doped tin oxide (FTO)/glass, and sapphire (Al_2O_3) substrates, which has not yet been demonstrated (Supporting Information, Figure S3).

Figure 3a shows the change in the diameter of the TiO_2 nanotube films with various bias voltages from 30 to 200 V.

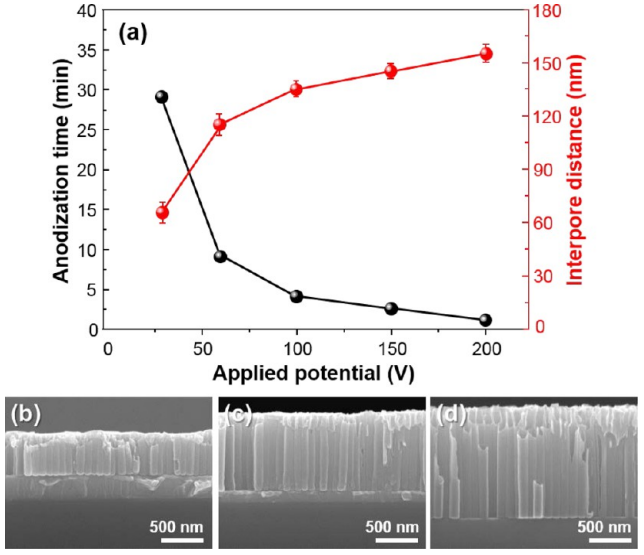

Figure 3. (a) Change in the diameter of TiO_2 nanotube films with various bias voltages from 30 to 200 V. (b) Cross-sectional SEM micrographs of the formation of TiO_2 nanotubes at 200 V for 30 s, (c) 60 s, and (d) 90 s.

The cross-sectional images clearly show that the nanotube diameter increases with increasing applied bias voltage (Supporting Information, Figure S4).[42] A close inspection revealed that the wall thickness saturates at relatively lower voltages, while the inner diameter still increases with the applied bias. As a result, the interpore distance of TiO_2 nanotube thin films versus the applied bias voltage shows fast increase at the lower voltages and gradual saturation at the higher voltages. The bias voltage has a significant impact on the anodization time. The anodization time was 29 min to achieve a 1.3-μm-thick nanotube film at 30 V but as short as 90 s at 200 V, shown in Figure 3b–d. This indicates that the higher bias voltage not only increases the electric field intensity of the Ti film but also speeds up the diffusion of ions, leading to the acceleration of the field-enhanced dissolution of Ti from the nanotubes. From cross-sectional SEM images, we have confirmed the termination time at which the Ti layer is completely converted to TiO_2 nanotubes. Current–time (I–t) curves cannot tell whether the anodization is finished or not

dx.doi.org/10.1021/jp405150b | J. Phys. Chem. C 2013, 117, 17824–17831

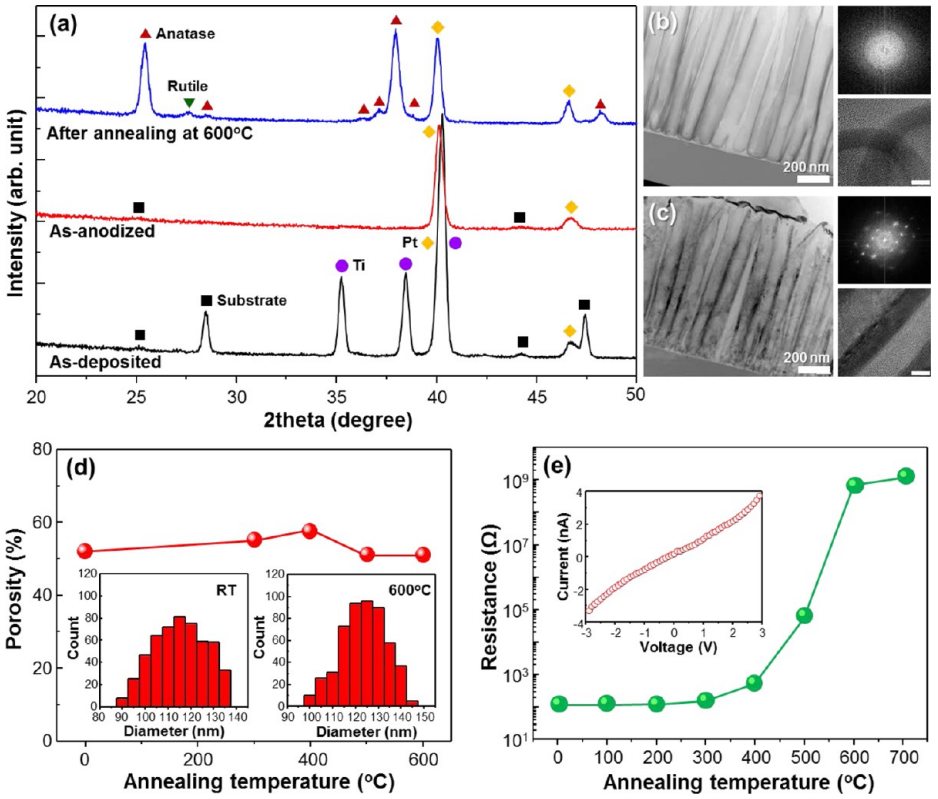

Figure 4. (a) Glancing angle X-ray diffraction patterns of a Ti/Si substrate, of a TiO_2 nanotube film on the substrate, and of a TiO_2 nanotube annealed at 600 °C for 5 h. The TEM images of TiO_2 nanotubes (b) for amorphous and (c) annealed at 600 °C. (d) Porosity change of TiO_2 nanotubes with different temperature. The insets show the histogram of a tube diameter. (e) Resistance change of a TiO_2 nanotube film was measured as a function of annealing temperature ranging from room temperature to 700 °C. The inset shows *I*−*V* characteristics of TiO_2 nanotube sensors at 600 °C in air.

due to large residual current between Pt IDEs and counter Pt (Figure S5, Supporting Information). Alternatively, it was possible to estimate the termination time, evaluating transparency. As Ti is converted into TiO_2 nanotubes, the color of the nanotube film becomes completely transparent. The point of the color being transparent is 90 s at the applied potential 200 V. Consequently, using the Pt as the current spreader, we could completely anodize the Ti film to TiO_2 nanotubes between the Pt IDEs and on the Pt IDEs (Supporting Information, Figure S6). We observed that nanotubes were well formed without disconnections at the edges of the Pt IDEs (Supporting Information, Figure S7).

The XRD patterns of the Ti film and anodized TiO_2 nanotube films before and after annealing at 600 °C are presented in Figure 4a. The as-anodized nanotube film does not exhibit any peak corresponding to the metallic Ti phase, which is a clear evidence for the complete conversion of the original Ti film to TiO_2 nanotubes. Since the as-anodized TiO_2 nanotubes are amorphous, as seen in the transmission electron microscopy (TEM) images in Figure 4b, no diffraction peaks are observed. After annealing, the XRD pattern shows the film to be predominantly composed of the anatase phase. The TEM images in Figure 4c show that the annealed TiO_2 nanotube film has high crystallinity with preferred orientations. The porosity of the TiO_2 nanotube films is estimated to be between 50% and 60% and is slightly affected by the annealing temperature (Figure 4d). The histogram of the tube diameter distribution shows a 10 nm increase of tube diameter due to the increase in the wall thicknesses (Supporting Information, Figure S8), which is attributed to an additional oxygen incorporation during the annealing at 600 °C. Resistance of the TiO_2 nanotube film was measured as a function of annealing temperature ranging from room temperature to 700 °C (Figure 4e). The resistance gradually increases and then dramatically rises after annealing at 500 and 600 °C, respectively. No noticeable changes in the resistance were observed upon annealing at 700 °C. In general, nonstoichiometry, a small variation of the composition, leads to a significant change of resistance in transition metal oxides. The as-anodized TiO_2 nanotubes are oxygen deficient with the existence of oxygen vacancies.[43] Since the oxygen vacancies are electron donors, the as-anodized TiO_2 nanotubes are highly conducting due to the degeneracy of electron carriers from the oxygen vacancies. After annealing in air, the oxygen vacancies are annihilated with the incorporation of oxygen atoms from the atmosphere, resulting in the increase in the resistance. This indicates that a metal−semiconductor transition was accomplished by annealing at 500−600 °C. The near linear current−voltage curve for the annealed TiO_2 nanotube film at 600 °C implies an ohmic contact behavior between TiO_2 and Pt IDEs.

This experimental work revealed the following important findings. (i) By clamping the Pt IDEs for anodization, the whole area of the Ti film is converted to TiO_2 nanotubes without an unreacted region. (ii) Since current efficiently spreads though the underlying Pt IDEs, the Ti layer is completely anodized to uniform TiO_2 nanotubes. (iii) The formation of TiO_2 nanotubes strongly depends on the grain size and crystallinity of the initial Ti film. Highly ordered

dx.doi.org/10.1021/jp405150b | J. Phys. Chem. C 2013, 117, 17824−17831

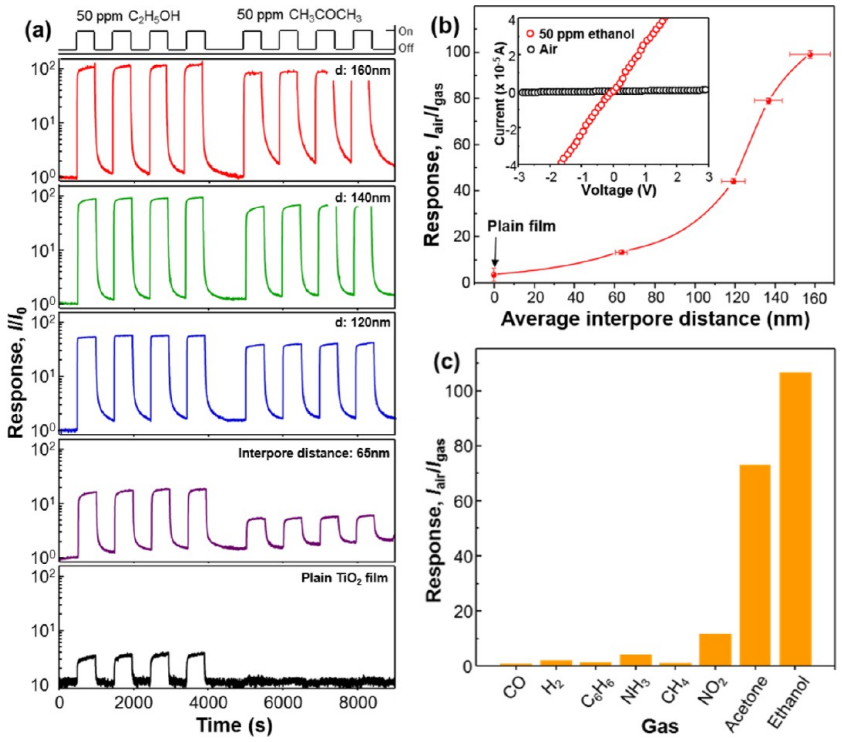

Figure 5. (a) Response curve of the reference dense-planar TiO_2 film and TiO_2 nanotube film prepared with different interpore distance to 50 ppm ethanol and acetone at 400 °C. The response for ethanol and acetone gases is presented as the nomarlized current I/I_0. (b) Response change of dense-planar TiO_2 film and TiO_2 nanotube film to 50 ppm ethanol gas at 400 °C. The inset shows the $I-V$ characteristics of the TiO_2 nanotube sensor in 50 ppm ethanol gas at 400 °C. (c) Response of the TiO_2 nanotube sensor to various gases.

nanotubes could be obtained from the anodization of the columnar Ti film deposited at 600 °C. (iv) At a bias voltage at 200 V, the anodization time is as short as 90 s for 1-μm-thick nanotube films. (v) Our approach is a synthesis-in-place method rather than synthesis-and-place methods. The resulting high-quality TiO_2 nanotube films on Pt-IDE-patterned SiO_2/Si substrates are suitable for use as chemiresistors without additional processes.

The gas sensing properties of the TiO_2 nanotube films with Pt IDEs were investigated after annealing at 600 °C. Figure 5a displays the typical response curves of TiO_2 nanotube films with different interpore distance toward 50 ppm ethanol and acetone at 400 °C. The response curves are presented with the normalized current I/I_0. The base resistance of TiO_2 nanotube sensors in air was about 1.0×10^9 Ω. Though anodization voltage increases, there were no significant differences in the resistance. The base resistance of TiO_2 nanotube sensors ranged from approximately 9.6×10^8 Ω to 1.3×10^9 Ω. Upon exposure to ethanol and acetone, the TiO_2 nanotube films quickly responded with a decrease in resistance, which revealed the typical n-type sensing behaviors of the films. The mechanism of ethanol sensor based on the TiO_2 nanotube can be accounted for by the surface-depletion model.[44] When the TiO_2 nanotube sensor is exposed to dry air, oxygen ions will be adsorbed onto the nanotube surface. Therefore, the depletion region may extend throughout the whole region of the TiO_2 nanotube, which results in high resistivity. However, upon exposure to reducing gas such as ethanol, ethanol molecules will react with the chemisorbed oxygen ions at the TiO_2 nanotube surface to form CO_2 and H_2O

$$CH_3CH_2OH\ (gas) \rightarrow CH_3CH_2OH\ (ads) \quad (1)$$

$$CH_3CH_2OH\ (ads) + 6O^-\ (ads) \rightarrow 2CO_2\ (gas) + 3H_2O\ (gas) + 6e^- \quad (2)$$

This leads to an increase in charge carrier concentration in the TiO_2 nanotube walls and a decrease in the surface depletion region width, which leads to a decrease (increase) in the resistance (conductivity) of the TiO_2 nanotube sensors.

For comparison, the response curve of a reference dense-planar TiO_2 film is also displayed. Compared to the reference dense-planar TiO_2 film, all the TiO_2 nanotube films show higher responses to ethanol and acetone. The 90% recovery time, the time for the sensor's initial resistance to reach 90% of its steady-state value for the nanotube film sensor, is about 710 s, which is much slower than that of the dense-planar sensor because desorbed gas molecules cannot be easily removed off from the nanotube surfaces. The gas response is enhanced as the interpore distance is increased from 60 to 160 nm. The drastic increase of response for the interpore distance of 160 nm, as plotted in Figure 5b, indicates that the interpore distance becomes sufficiently large for the easy access of gaseous molecules into the bottom of the nanotubes (Supporting Information, Figure S9). This suggests that controlling the interpore distance as well as increasing the surface-to-volume ratio is a key factor to enhance the gas response. The maximum response of ethanol is as large as 106, which is much higher than those previously reported for high sensitivity sensors based on TiO_2 nanoparticles (10−100 ppm ethanol and 6−100 ppm acetone at 400 °C),[18] TiO_2 nanobelts (41−500 ppm ethanol at 200 °C),[22] TiO_2 nanorods (17−400 ppm ethanol at 500 °C),[45] TiO_2 hollow hemispheres (71−50 ppm ethanol at 250 °C),[16] and TiO_2 nanotubes (15−47 ppm ethanol at 500 °C).[46] Although several reports have

dx.doi.org/10.1021/jp405150b | J. Phys. Chem. C 2013, 117, 17824−17831

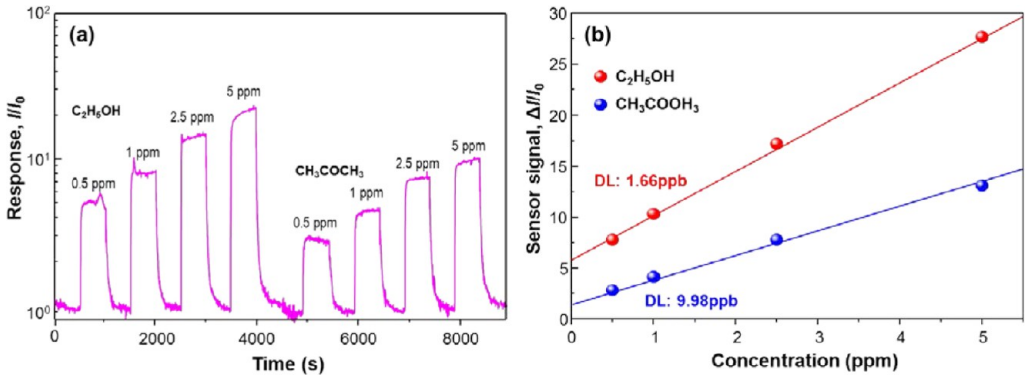

Figure 6. (a) Response curve of the TiO_2 nanotube sensors to 0.5−5 ppm ethanol and acetone at an applied bias voltage of 1 V. (b) Detection limits of TiO_2 nanotube sensor to ethanol and acetone.

commented on the importance of nanotubular structures in enhancing the gas-sensing performance of metal oxide materials,[36,47] no such enhancement in gas sensitivity by varying the nanotube diameter has yet been reported.

The TiO_2 nanotube (the interpore distance of 160 nm) sensor exhibits much higher response toward ethanol and acetone than toward CO, H_2, C_6H_6, NH_3, CH_4, and NO_2 gases (Figure 5c). This indicates the nanotube sensor is beneficial for the selective detection of acetone and ethanol. To evaluate the detection limits of the sensor to ethanol and acetone, the response of the nanotube sensor was measured over a range of 0.5−5 ppm, as plotted in Figure 6a. The responses of the nanotube sensor are 6.75, 10.74, 21.25, and 31.31 to 0.5, 1, 2.5, and 5 ppm ethanol and 4.07, 6.25, 10.62, and 14.61 to 0.5, 1, 2.5, and 5 ppm acetone, respectively. Although the 0.5 ppm concentration was the lowest experimentally examined in the present study, the theoretical detection limit[48,49] (signal-to-noise ratio >3) was calculated to be approximately 1.6 ppb for ethanol and 9.98 ppb for acetone (Figure 6b). Since acetone and ethanol are found in the breath of patients with diabetes mellitus (acetone 0.1−10 ppm) or lung cancer (ethanol 50−2000 ppb),[50] we suggest that our TiO_2 nanotube sensors have promising potential for application in breath analyzers used for the early diagnosis of such diseases.

CONCLUSION

We have developed a synthesis-in-place method for synthesizing highly ordered TiO_2 nanotube films. Using the method, unprecedentedly well-ordered TiO_2 nanotube films could be directly synthesized on the patterned Si, glass, or sapphire substrates and then used for chemiresistors without additional fabrication processes. Our TiO_2 nanotube sensors exhibited extremely high and selective responses to ethanol and acetone. The detection limits of several parts per billion to ethanol and acetone suggest the promising potential of the nanotube sensors for application in breath analyzers used for the early diagnosis of human diseases. We believe that our synthesis-in-place method will broaden the use of TiO_2 nanotubes and nanofilms to improve the performance of various devices including chemiresistors, batteries, solar cells, and solar water splitting cells. In principle, the method is applicable to other materials such as Al_2O_3,[51] ZrO_2,[52] WO_3,[53] Nb_2O_5,[54] Fe_2O_3,[55] and Ta_2O_5[56] to form nanotubular films.

EXPERIMENTAL SECTION

Sensor Fabrication. The 200-nm-thick Pt films were prepared on SiO_2/Si substrate using an electron beam evaporator. Prior to Pt deposition, 50-nm-thick Ti was deposited to utilize the excellent adhesion of Pt to the SiO_2/Si substrate. Pt IDEs in which the gap between each electrode was 5 μm were fabricated using photolithography and dry etching. After patterning the Pt IDEs, a 500-nm-thick Ti film was deposited onto the predefined regions by a shadow mask on the Pt-IDE-patterned SiO_2/Si substrate using an electron beam evaporator (Rocky Mountain Vacuum Tech.) at 600 °C. A base pressure was maintained in the range of 10^{-6} Torr. Applied e-beam voltage and current were set at 7.3 kV and 100 mA, respectively, leading to a deposition rate of 1.0 Å/s. Anodization was carried out in a two-electrode electrochemical system at room temperature. The electrolyte was ethylene glycol (99.5% purity, Junsei) solution with 0.3 wt % of NH_4F (99.5% purity, Junsei) and 3 vol % water, and a voltage of 30−200 V was applied between a platinum cathode and a titanium film anode. Anodization durations of 1.5−30 min resulted in films comprised of a 1-μm-thick nanotubular structure. After anodization, the samples were carefully washed with distilled water and dried in nitrogen. After anodization, the samples were annealed at 600 °C for 5 h in ambient air to induce the amorphous to anatase phase transition.

Material Characterization. The morphologies of the synthesized TiO_2 nanotube films were characterized by scanning electron microscopy (FEI, XL30 FEG ESEM) using 15 kV voltages. TEM images were taken by a JEOL JEM 2100F with a probe-Cs corrector. Cross-sectional TEM specimens of TiO_2 nanotubes on a SiO_2/Si substrate were prepared by mechanical polishing followed by ion milling with Ar ions. The crystallinity and phase of the sensor films were characterized by glancing angle XRD (D/Max-2500, Rigaku), where Cu Kα radiation (wavelength = 1.5418 Å) was used for the X-ray source and the incident angle was fixed at a small angle (2°). For all the TiO_2 sensing films, selected area electron diffraction patterns from TEM and XRD patterns could be indexed with a pure anatase phase of TiO_2 with lattice constants of a = 3.7822 Å and c = 9.5023 Å (JCPDS #84-1286). The resistivities of the TiO_2 nanotube films were measured using the two-probe DC method (Keithley 236) as a function of annealing temperature.

Sensor Measurements. The sensing properties of the synthesized TiO_2 nanotube film sensors were measured at 400 °C. The flow gas was changed from dry air to a calibrated target gas (balanced with dry air, Sinyang Gases), under a DC bias

dx.doi.org/10.1021/jp405150b | J. Phys. Chem. C 2013, 117, 17824−17831

voltage of 1 V using a source measurement unit (Keithley 236). A constant flow rate of 1000 sccm was used for the dry air and target gas. The current−voltage characteristics of the TiO_2 nanotube film sensors were almost linear near 1 V, indicating a very small contribution of the contact resistance to the overall performance. The response of the sensors ($\Delta I/I_0$ for ethanol, acetone, CO, H_2, C_6H_6, NH_3, CH_4, and NO_2) was accurately determined by measuring the baseline resistances of the sensors in dry air and the fully saturated resistances after exposure to the test gas. The gas flow was controlled using mass flow controllers, and all measurements were recorded on a computer by using LabVIEW over the GPIB interface. The current−voltage characteristics of the sensors were measured to check the contribution of the contact resistance between Pt IDEs and the TiO_2 nanotube film to the overall performance.

■ ASSOCIATED CONTENT

Supporting Information

Detailed information about the structures, morphologies, and gas sensing properties of TiO_2 nanotube thin films. This material is available free of charge via the Internet at http://pubs.acs.org.

■ AUTHOR INFORMATION

Corresponding Author

*E-mail: hwjang@snu.ac.kr.

Notes

The authors declare no competing financial interest.

■ ACKNOWLEDGMENTS

This work was financially supported by a research program of the Korea Institute of Science and Technology, the Core Technology of Materials Research and Development Program, and a research program of the Korea Ministry of Environment. H.W.J. acknowledges the financial support of the Fusion Research Program for Green Technologies and the Outstanding Young Researcher Program through the National Research Foundation of Korea.

■ REFERENCES

(1) Linsebigler, A. L.; Lu, G. Q.; Yates, J. T. Photocatalysis on TiO_2 Surfaces: Principle, Mechanisms, and Selected Results. *Chem. Rev.* **1995**, *95*, 735−758.

(2) Asahi, R.; Morikawa, T.; Ohwaki, T.; Aoki, K.; Taga, Y. Visible-Light Photocatalysis in Nitrogen-Doped Titanium Oxides. *Science* **2001**, *293*, 269−271.

(3) Diebold, U. Structure and Properties of TiO_2 Surface: A Brief Review. *Appl. Phys. A* **2003**, *76*, 681−687.

(4) Zhuge, F. W.; Qiu, J. J.; Li, X. M.; Gao, X. D.; Gan, X. Y.; Yu, W. D. Toward Hierarchical TiO_2 Nanotube Arrays for Efficient Dye-Sensitized Solar Cells. *Adv. Mater.* **2011**, *23*, 1330−1334.

(5) Bach, U.; Lupo, D.; Comte, P.; Moser, J. E.; Weissortel, F.; Salbeck, J.; Spreitzer, H.; Gratzel, M. Solid-State Dye-Sensitized Mesoporous TiO_2 Solar Cells with High Photon-to-Electron Conversion Efficiencies. *Nature* **1998**, *395*, 583−585.

(6) Oregan, B.; Gratzel, M. A Low-Cost, High-Efficiency Solar Cell Based on Dye-Sensitized Colloidal TiO_2 Films. *Nature* **1991**, *353*, 737−740.

(7) Khan, S. U. M.; Al-Shahry, M.; Ingler, W. B. Efficient Photochemical Water Splitting by a Chemically Modified n-TiO_2. *Science* **2002**, *297*, 2243−2245.

(8) Park, J. H.; Kim, S.; Bard, A. J. Novel Carbon-Doped TiO_2 Nanotube Arrays with High Aspect Ratios for Efficient Solar Water Splitting. *Nano Lett.* **2006**, *6*, 24−28.

(9) Liu, G.; Yang, H. G.; Wang, X. W.; Cheng, L. N.; Pan, J.; Lu, G. Q.; Cheng, H. M. Visible Light Responsive Nitrogen Doped Anatase TiO_2 Sheets with Dominant {001} Facets Derived From TiN. *J. Am. Chem. Soc.* **2009**, *131*, 12868−12869.

(10) Zhang, X. T.; Sato, O.; Taguchi, M.; Einaga, Y.; Murakami, T.; Fujishima, A. Self-Cleaning Particle Coating with Antireflection Properties. *Chem. Mater.* **2005**, *17*, 696−700.

(11) Zhang, X. T.; Fujishima, A.; Jin, M.; Emeline, A. V.; Murakami, T. Double-Layered TiO_2-SiO_2 Nanostructured Films with Self-Cleaning and Antireflective Properties. *J. Phys. Chem. B* **2006**, *110*, 25142−25148.

(12) Boukennous, Y.; Benyahia, B.; Charif, M. R.; Chikouche, A. Antireflection Coating of TiO_2 Study and Deposition by the Screen Printing Method. *J. Phys. III* **1995**, *5*, 1297−1305.

(13) Ortiz, G. F.; Hanzu, I.; Djenizian, T.; Lavela, P.; Tirado, J. L.; Knauth, P. Alternative Li-Ion Battery Electrode Based on Self-Organized Titania Nanotubes. *Chem. Mater.* **2009**, *21*, 63−67.

(14) Huang, S. Y.; Kavan, L.; Exnar, I.; Gratzel, M. Rocking Chair Lithium Battery Based on Nanocrystalline TiO_2 (Anatase). *J. Electrochem. Soc.* **1995**, *142*, L142−L144.

(15) Wagemaker, M.; Kentgens, A. P. M.; Mulder, F. M. Equilibrium Lithium Transport between Nanocrystalline Phases in Intercalated TiO_2 Anatase. *Nature* **2002**, *418*, 397−399.

(16) Moon, H. G.; Shim, Y. S.; Su, D.; Park, H. H.; Yoon, S. J.; Jang, H. W. Embossed TiO_2 Thin Films with Tailored Links between Hollow Hemispheres: Synthesis and Gas-Sensing Properties. *J. Phys. Chem. C* **2011**, *115*, 9993−9999.

(17) Tang, H.; Prasad, K.; Sanjines, R.; Levy, F. TiO_2 Anatase Thin Films as Gas Sensors. *Sens. Actuators, B* **1995**, *26*, 71−75.

(18) Rella, R.; Spadavecchia, J.; Manera, M. G.; Capone, S.; Taurino, A.; Martino, M.; Caricato, A. P.; Tunno, T. Acetone and Ethanol Solid-State Gas Sensors Based on TiO_2 Nanoparticles Thin Film Deposited by Matrix Assisted Pulsed Laser Evaportation. *Sens. Actuators, B* **2007**, *127*, 426−431.

(19) Bavykin, D. V.; Friedrich, J. M.; Walsh, F. C. Protonated Titanates and TiO_2 Nanostructured Materials: Synthesis, Properties, and Applications. *Adv. Mater.* **2006**, *18*, 2807−2824.

(20) Law, M.; Greene, L. E.; Johnson, J. C.; Saykally, R.; Yang, P. D. Nanowire Dye-Sensitized Solar Cells. *Nat. Mater.* **2005**, *4*, 455−459.

(21) Burnside, S. D.; Shklover, V.; Barbe, C.; Comte, P.; Arendse, F.; Brooks, K.; Gratzel, M. Self-Organization of TiO_2 Nanoparticles in Thin Films. *Chem. Mater.* **1998**, *10*, 2419−2425.

(22) Hu, P. Q.; Du, G. J.; Zhou, W. J.; Cui, J. J.; Lin, J. J.; Liu, H.; Liu, D.; Wang, J. Y.; Chen, S. W. Enhancement of Ethanol Vapor Sensing of TiO_2 Nanobelts by Surface Engineering. *ACS. Appl. Mater. Interfaces* **2010**, *2*, 3263−3269.

(23) Liu, B.; Aydil, E. S. Growth of Oriented Single-Crystalline Rutile TiO_2 Nanorods on Transparent Conducting Substrates for Dye-Sensitized Solar Cells. *J. Am. Chem. Soc.* **2009**, *131*, 3985−3990.

(24) Yang, H. G.; Liu, G.; Qiao, S. Z.; Sun, C. H.; Jin, Y. G.; Smith, S. C.; Zou, J.; Cheng, H. M.; Lu, G. Q. Solvothermal Synthesis and Photoreactivity of Anatase TiO_2 Nanosheets with Dominant {001} Facets. *J. Am. Chem. Soc.* **2009**, *131*, 4078−4083.

(25) Mor, G. K.; Shankar, K.; Paulose, M.; Varghese, O. K.; Grimes, C. A. Use of Highly-Ordered TiO_2 Nanotube Arrays in Dye-Sensitized Solar Cells. *Nano Lett.* **2006**, *6*, 215−218.

(26) Zuruzi, A. S.; MacDonald, N. C. Facile Fabrication and Integration of Patterned Nanostructured TiO_2 for Microsystems Applications. *Adv. Funct. Mater.* **2005**, *15*, 396−402.

(27) Zuruzi, A. S.; MacDonald, N. C.; Moskovits, M.; Kolmakov, A. Metal Oxide "Nanosponges" as Chemical Sensors: Highly Sensitive Detection of Hydrogen using Nanosponge Titania. *Angew. Chem., Int. Ed.* **2007**, *46*, 4298−4301.

(28) Zuruzi, A. S.; Kolmakov, A.; MacDonald, N. C.; Moskovits, M. Highly Sensitive Gas Sensor Based on Integrated Titania Nanosponge Arrays. *Appl. Phys. Lett.* **2006**, *88*, 102904.

(29) Kasuga, T.; Hiramatsu, M.; Hoson, A.; Sekino, T.; Niihara, K. Formation of Titanium Oxide Nanotube. *Langmuir* **1998**, *14*, 3160−3163.

(30) Zhu, K.; Neale, N. R.; Miedaner, A.; Frank, A. J. Enhanced Charge-Collection Efficiencies and Light Scattering in Dye-Sensitized Solar Cells Using Oriented TiO_2 Nanotubes Arrays. *Nano Lett.* **2007**, *7*, 69−74.
(31) Macak, J. M.; Tsuchiya, H.; Schmuki, P. High-Aspect-Ratio TiO_2 Nanotubes by Anodization of Titanium. *Angew. Chem., Int. Ed.* **2005**, *44*, 2100−2102.
(32) Macak, J. M.; Tsuchiya, H.; Taveira, L.; Aldabergerova, S.; Schmuki, P. Smooth Anodic TiO_2 Nanotubes. *Angew. Chem., Int. Ed.* **2005**, *44*, 7463−7465.
(33) Varghese, O. K.; Paulose, M.; Grimes, C. A. Long Vertically Aligned Titania Nanotubes on Transparent Conducting Oxide for Highly Efficient Solar Cells. *Nat. Nanotechnol.* **2009**, *4*, 592−597.
(34) Grimes, C. A. Synthesis and Application of Highly Ordered Arrays of TiO_2 Nanotubes. *J. Mater. Chem.* **2007**, *17*, 1451−1457.
(35) Zheng, Q.; Zhou, B. X.; Bai, J.; Li, L. H.; Jin, Z. J.; Zhang, J. L.; Li, J. H.; Liu, Y. B.; Cai, W. M.; Zhu, X. Y. Self-Organized TiO_2 Nanotube Array Sensor for The Determination of Chemical Oxygen Demand. *Adv. Mater.* **2008**, *20*, 1044−1049.
(36) Lin, S. W.; Li, D. R.; Wu, J.; Li, X. G.; Akbar, S. A. A Selective Room Temperature Formaldehyde Gas Sensor using TiO_2 Nanotube Arrays. *Sens. Actuators, B* **2011**, *156*, 505−509.
(37) Han, C. H.; Hong, D. W.; Kim, I. J.; Gwak, J.; Han, S. D.; Singh, K. C. Synthesis of Pd or Pt/Titanate Nanotube and Its Application to Catalytic Type Hydrogen Gas Sensor. *Sens. Actuators, B* **2007**, *128*, 320−325.
(38) Seo, M. H.; Yuasa, M.; Kida, T.; Huh, J. S.; Yamazoe, N.; Shimanoe, K. Microstructure Control of TiO_2 Nanotubular Films for Improved VOC Sensing. *Sens. Actuators, B* **2011**, *154*, 251−256.
(39) Mor, G. K.; Varghese, O. K.; Paulose, M.; Grimes, C. A. Transparent Highly Ordered TiO_2 Nanotube Arrays via Anodization of Titanium Thin Films. *Adv. Funct. Mater.* **2005**, *15*, 1291−1296.
(40) Lei, B. X.; Liao, J. Y.; Zhang, R.; Wang, J.; Su, C. Y.; Kuang, D. B. Ordered Crystalline TiO_2 Nanotube Arrays on Transparent FTO Glass for Efficient Dye-Sensitized Solar Cells. *J. Phys. Chem. C* **2010**, *114*, 15228−15233.
(41) Roy, P.; Berger, S.; Schmuki, P. TiO_2 Nanotubes: Synthesis and Applications. *Angew. Chem., Int. Ed.* **2011**, *50*, 2904−2939.
(42) Bauer, S.; Pittrof, A.; Tsuchiya, H.; Schmuki, P. Size-Effect in TiO_2 Nanotubes: Diameter Dependent Anatase/Rutile Stabilication. *Electrochem. Commun.* **2011**, *13*, 538−541.
(43) Shin, J. Y.; Joo, J. H.; Samuelis, D.; Maier, J. Oxygen-Deficient $TiO_{2-\delta}$ Nanoparticles via Hydrogen Reduction for High Rate Capability Lithium Batteries. *Chem. Mater.* **2012**, *24*, 543−551.
(44) Feng, P.; Wan, Q.; Wang, T. H. Contact-Controlled Sensing Properties of Flowerlike ZnO Nanostructures. *Appl. Phys. Lett.* **2005**, *87*, 213111.
(45) Singh, S.; Kaur, H.; Singh, V. N.; Jain, K.; Senguttuvan, T. D. Highly Sensitive and Pulse-Like Response Towoard Ethanol of Nb Doped TiO_2 Nanotubes Based on Gas Sensors. *Sens. Actuators, B* **2012**, *171*, 899−906.
(46) Seo, M. H.; Yuasa, M.; Kida, T.; Huh, J. S.; Shimanoe, K.; Yamazoe, N. Gas Sensing Characteristics and Porosity Control of Nanostructured Films Composed of TiO_2 Nanotubes. *Sens. Actuators, B* **2009**, *137*, 513−520.
(47) Perillo, P. M.; Rodriguez, D. F. The Gas Sensing Properties at Room Temperature of TiO_2 Nanotubes by Anodization. *Sens. Actuators, B* **2012**, *171*, 639−643.
(48) Dua, V.; Surwade, S. P.; Ammu, S.; Agnihotra, S. R.; Jain, S.; Roberts, K. E.; Park, S.; Ruoff, R. S.; Manohar, S. K. All-Organic Vapor Sensor Using Inkjet-Printed Reduced Graphene Oxide. *Angew. Chem., Int. Ed.* **2010**, *49*, 2154−2157.
(49) Li, J.; Lu, Y. J.; Ye, Q.; Cinke, M.; Han, J.; Meyyappan, M. Carbon Nanotube Sensors for Gas and Organic Vapor Detection. *Nano Lett.* **2003**, *3*, 929−933.
(50) Machado, R. F.; Laskowski, D.; Deffenderfer, O.; Burch, T.; Zheng, S.; Mazzone, P. J.; Mekhail, T.; Jennings, C.; Stoller, J. K.; Pyle, J.; Duncan, J.; Dweik, R. A.; Erzurum, S. C. Detection of Lung Cancer by Sensor Array Analyses of Exhaled Breath. *Am. J. Respir. Crit. Care* **2005**, *171*, 1286−1291.
(51) Diggle, J. W.; Downie, T. C.; Goulding, C. W. Anodic Oxide Films on Aluminum. *Chem. Rev.* **1969**, *69* (3), 365−405.
(52) Tsuchiya, H.; Macak, J. M.; Sieber, I.; Schmuki, P. Self-Organized High-Aspect-Ratio Nanoporous Zirconium Oxides Prepared by Electrochemical Anodization. *Small* **2005**, *1*, 722−725.
(53) Tsuchiya, H.; Macak, J. M.; Sieber, I.; Taveira, L.; Ghicov, A.; Sirotna, K.; Schmuki, P. Self-Organized Porous WO_3 Formed in NaF Electrolytes. *Electrochem. Commun.* **2005**, *7*, 295−298.
(54) Sieber, I.; Hildebrand, H.; Friedrich, A.; Schmuki, P. Formation of Self-Organized Niobium Porous Oxide on Niobium. *Electrochem. Commun.* **2005**, *7*, 97−100.
(55) Mohapatra, S. K.; John, S. E.; Banerjee, S.; Misra, M. Water Photooxidation by Smooth and Ultrathin α-Fe_2O_3 Nanotube Arrays. *Chem. Mater.* **2009**, *21*, 3048−3055.
(56) Wei, W.; Macak, J. M.; Schmuki, P. High Aspect Ratio Ordered Nanoporous Ta_2O_5 Films by Anodization of Ta. *Electrochem. Commun.* **2008**, *10*, 428−432.